AD-A140 569 THIN FILM MODELS OF SMSI (SHOW STRONG METAL-SUPPORT INTERACTIONS) CATALYS.. (U) TEXAS UNIV AT AUSTIN DEPT OF CHEMISTRY D N BELTYON ET AL. 17 OCT 83 TR-30 1/1

UNCLASSIFIED N00014-75-C-0922 F/G 20/12 NL

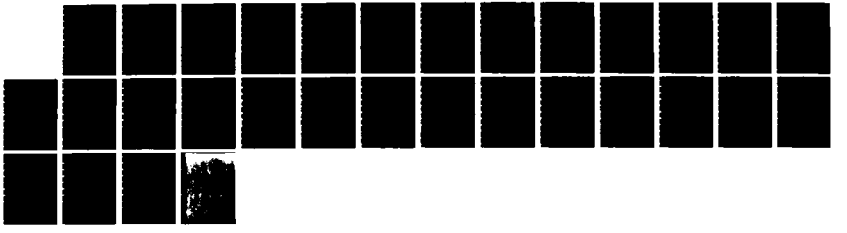

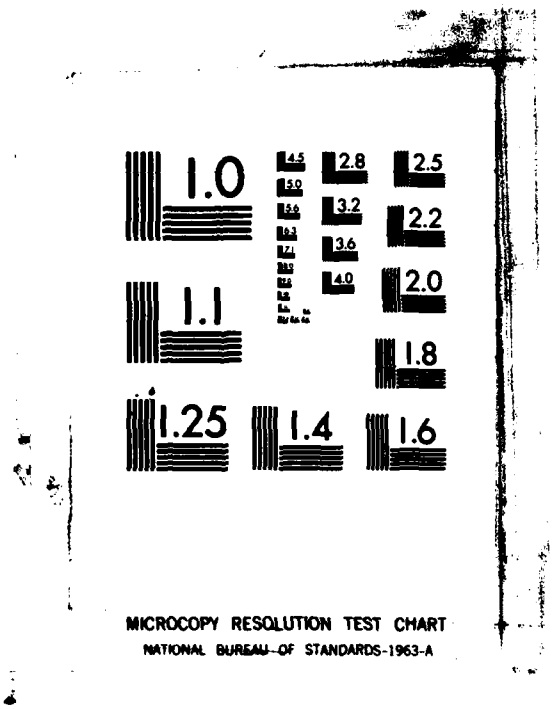
1.0
1.1
1.25
1.4
1.6
1.8
2.0
2.2
2.5
2.8
3.2
3.6
4.0
4.5
5.0
5.6
6.3
7.1
8.0
9.0
MICROCOPY RESOLUTION TEST CHART
NATIONAL BUREAU OF STANDARDS-1963-A

OFFICE OF NAVAL RESEARCH

Contract N00014-75-C-0922

Task No. NR 056-578

TECHNICAL REPORT NO. 30

Thin Film Models of SMSI Catalysts: Pt on Oxidized Titanium

by

D. N. Belton, Y.-M. Sun and J. M. White

Prepared for publication

in

The Journal of Physical Chemistry

Department of Chemistry

University of Texas at Austin

Austin, Texas 78712

October 17, 1983

SECURITY CLASSIFICATION OF THIS PAGE (When Data Entered)

REPORT DOCUMENTATION PAGE

READ INSTRUCTIONS BEFORE COMPLETING FORM

1. REPORT NUMBER	2. GOVT ACCESSION NO. AD A140569
3. RECIPIENT'S CATALOG NUMBER	
4. TITLE (and Subtitle) Thin Film Models of SMSI Catalysts: Pt on Oxidized Titanium	5. TYPE OF REPORT & PERIOD COVERED Technical Report 30 Jan. 1 - Dec. 31, 1983
	6. PERFORMING ORG. REPORT NUMBER
7. AUTHOR(s) D. N. Belton, Y.-M. Sun and J. M. White	8. CONTRACT OR GRANT NUMBER(s) N00014-75-C-0922
9. PERFORMING ORGANIZATION NAME AND ADDRESS J. M. White Dept. of Chemistry, University of Texas Austin, TX 78712	10. PROGRAM ELEMENT, PROJECT, TASK AREA & WORK UNIT NUMBERS Project NR-056-578
11. CONTROLLING OFFICE NAME AND ADDRESS Department of the Navy Office of Naval Research Arlington, VA 22217	12. REPORT DATE October 17, 1983
	13. NUMBER OF PAGES 26
14. MONITORING AGENCY NAME & ADDRESS(if different from Controlling Office)	15. SECURITY CLASS. (of this report)
	15a. DECLASSIFICATION/DOWNGRADING SCHEDULE

16. DISTRIBUTION STATEMENT (of this Report)

Approved for public release: Distribution unlimited.

17. DISTRIBUTION STATEMENT (of the abstract entered in Block 20, if different from Report)

18. SUPPLEMENTARY NOTES

Preprint: Accepted, The Journal of Physical Chemistry

19. KEY WORDS (Continue on reverse side if necessary and identify by block number)

20. ABSTRACT (Continue on reverse side if necessary and identify by block number)

Thin films of Pt, vapor deposited on an oxidized Ti foil, have been utilized as models of high surface area Pt/TiO_2 catalysts which show strong metal support interactions. As a function of Pt coverage, the development of bulk Pt chemisorption characteristics occurs at significantly lower coverages on the oxidized substrate. At a given Pt coverage there is less chemisorption of both CO & H_2 on the reduced, as compared to the oxidized, TiO_2 and the desorption spectra peak at lower temperatures. We propose a model in

DD FORM 1 JAN 73 1473 EDITION OF 1 NOV 65 IS OBSOLETE
S/N 0102-014-6601 |

SECURITY CLASSIFICATION OF THIS PAGE (When Data Entered)

20. which the morphology of the Pt on the reduced catalysts is significantly flatter (dominated by (111) terraces) and is slightly modified electronically, as compared to the oxidized sample.

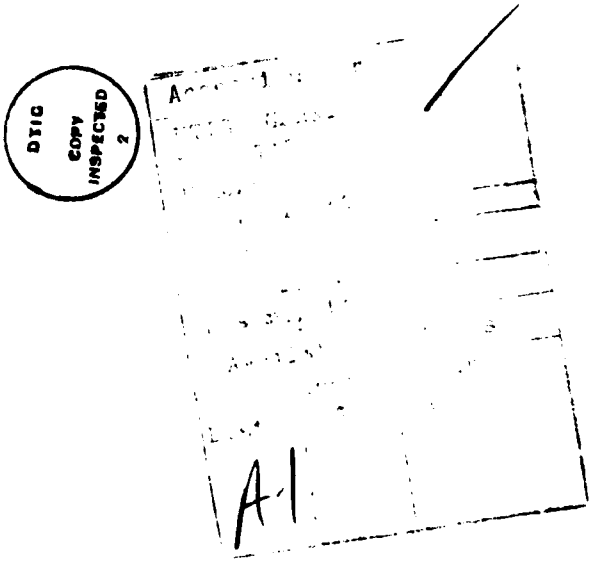

Thin Film Models of SMSI Catalysts: Pt on Oxidized Titanium*

D. N. Belton, Y.-M. Sun and J. M. White

Department of Chemistry

University of Texas

Austin, TX 78712

* Supported in part by the Office of Naval Research.

Abstract

Thin films of Pt, vapor deposited on an oxidized Ti foil, have been utilized as models of high surface area Pt/ TiO_2 catalysts which show strong metal-support interactions (SMSI). Both fully oxidized($Ti^{(4+)}$) and partially reduced(significant amounts of $Ti^{(3+)}$) surfaces were studied. As a function of Pt coverage, the development of bulk Pt chemisorption characteristics occurs at significantly lower coverages on the oxidized substrate. In particular, at a given Pt coverage there is less chemisorption of both CO and H_2 on the reduced, as compared to the oxidized, TiO_2 and the desorption spectra peak at lower temperatures. No evidence for significant differences in the chemical state of the Pt is found by XPS and AES. We propose a model, consistent with earlier work on high surface area Pt/TiO_2 catalysts, in which the morphology of the Pt on the reduced catalysts is significantly flatter (dominated by (111) terraces) and is slightly modified electronically, as compared to the oxidized sample.

Introduction.

Since the detailed report by Tauster et al.[1,2] of strong metal support interactions (SMSI) in several systems, the cause of this interesting effect has been an area of great activity in the surface science-catalysis community. SMSI is characterized by the loss of a supported metal's ability to chemisorb CO and H_2. Explanations such as metal particle morphology, surface contaminants, encapsulation of metal particles by the support, and charge transfer between metal and support have been proposed to explain the phenomena. Experiments conducted on metal impregnated oxide powders, the actual catalyst, have been unable to control unambiguously many of the system variables and thus have been unable to determine the cause(s) for SMSI. UHV studies on models for these catalysts have most often explored the electronic structure of the system through electron spectroscopy. This approach has sometimes led to the conclusion that electrons are transferred from the support to the metal,[3-5] but without the supporting chemisorption studies it is impossible to assign this charge transfer as the cause of SMSI.

In the experiments presented here we model the Pt/TiO_2 catalyst (both SMSI and non-SMSI) in UHV. The model consists of various amounts of Pt deposited on a thin film($\approx 50A^{o}$) of TiO_2. These thin films and the supporting oxide were characterized using X-ray photoelectron spectroscopy (XPS) and Auger electron spectroscopy (AES). Thermal desorption spectroscopy (TDS) of two different adsorbates, H_2 and CO, was examined and correlated with the XPS data.

Experimental

The experiments were done with a modified PHI 548 photoelectron spectrometer that has been described eleswhere.[6] The system pressure was typically in $3x10^{-10}$ Torr. XPS spectra were taken using a Vacuum Generators dual anode (Mg and Al) x-ray source, operating the Mg anode at 240 Watts. The cylindrical mirror analyzer (CMA) was operated in the retard mode at 25 eV pass energy. Thermal desorption spectra were obtained using a line-of-sight geometry with a multiplexed quadrupole mass spectrometer.

The titanium foil was mounted using Ta leads spotwelded to the back of the foil. The sample was heated resistively with a programmable DC power supply and was cooled to approximately 110K with liquid nitrogen cooling. A chromel-alumel thermocouple, spot-welded to the titanium foil, was used for temperature measurement. Surface impurities, such as C, Cl,and S, were removed by combined Ar^+ bombardment and high temperature oxidation.

The TiO_2 film was formed by dosing 4000L of O_2 at 625K. These oxidation conditions led to an oxide film that gave the XPS spectrum shown in Fig. 1. The observed Ti(2p) binding energies (BE) of 458.8 and 464.3 eV are indicative of TiO_2.[7] The narrow FWHM (1.9 eV) of the $Ti(2p_{3/2})$ peak indicates that the surface region is dominated by Ti^{4+} species. Using an electron mean free path of 11Å[8] for the Ti(2p) electrons we calculate a minimum thickness of 35Å for the TiO_2 film. Samples prepared in this manner are referred to as fully oxidized and are denoted TiO_2(ox).

To prepare a partially reduced TiO_2 sample, denoted TiO_2(red), the fully oxidized sample was heated in vacuum at 750K for about 5 minutes. Figure 1 shows the XPS spectrum of a typical TiO_2(red) sample. The obvious

low BE shoulder is due to the presence Ti^{3+}. Increased reduction time led to a concurrent increase in the intensity of this shoulder. An approximate decomposition of the peak shape indicates about 20% of the total Ti(2p) signal originates from Ti^{3+}. The method of reduction, heating in vacuum at relatively low temperatures, is expected to cause diffusion of oxygen into the Ti foil, leaving the surface region oxygen-deficient. Within this framework, the bulk of the TiO_2 film is more highly reduced than the surface suggesting that the actual surface concentration of Ti^{3+} is lower than 20%. Establishing an upper limit of Ti^{3+} concentration was not attempted due to the difficulties involved in estimating the distribution of Ti^{3+} as a function of distance from the surface.

Controlled amounts of Pt were vapor deposited onto the oxidized and reduced TiO_2 substrates. The Pt doser consisted of a resistively heated W filament wrapped with a 99.99% Pt wire. The temperature of the Pt was monitored with a W/5%Re-W/26%Re thermocouple and was typically held constant to within 3K at about 1600K. During Pt deposition, the oxidized foil substrate was placed approximately 3 cm from the doser and in a position that gave macroscopically uniform coverages over the oxide surface. A typical dose rate was 0.5 ML min^{-1} as determined by the time dependence of the relative Auger signals of Pt and Ti. This rate was easily varied by changing either doser temperature or sample position. No impurities were found by AES in the Pt overlayer. Figure 2 shows a typical AES spectrum for multilayer Pt on TiO_2. This quality was obtained only after considerable effort; deposition of C in the Pt overlayers was a particularly troublesome problem. Since surface carbon is known to suppress chemisorption,[9,10] it is very important that the Pt overlayer be free of it. Moreover, C buildup would lead to improper determination of the Pt overlayer thickness.

Results

Figure 3 shows the behavior of the Ti(387) and Pt(235) AES signals as a function of Pt dose with the substrate held at 300K. Data for deposition onto both the oxidized and reduced substrates are included. Growth curves based on an ideal (layer-by-layer) model are also shown. These curves are calculated as follows: When the first monolayer is complete, the Ti(387 eV) signal will be 0.58 of its initial value as calculated using[11]

$$I_{Ti}(d) = I_{Ti}^{o} \exp[-d/(\lambda_{Ti}\cos\theta)]$$

In this equation d is the thickness of 1 monolayer (ML) of Pt (2.41 Å), $I_{Ti}(d)$ the peak-to-peak height of the Ti(387) signal, I_{Ti}^{o} the initial 387 eV signal, λ_{Ti} the electron inelastic mean free path (8 Å for a 387 eV electron[8,12,13]), and θ the analyzer acceptance angle (50°). The Pt(235) signal for 1 ML of uniform coverage is calculated using a similar equation with λ_{Pt} = 7 Å. Although the assignment of mean free paths is not unambiguous, these values are reasonable choices for this system. Between 0 and 1 ML coverage, the signals are assumed to change linearly with Pt coverage. The same equations can be used to compute attentuation and growth for full development of N monolayers with linear segments between. These linear segments are shown in Fig. 3.

Examination of Fig. 3 shows the growth mode is nearly ideal for the first 3ML of Pt. The fact that the Ti AES points lie slightly below the calculated curve indicates that islanding with 3D particle formation is not dominant in this region. The deviation is probably due to choice of electron inelastic mean free path lengths since islanding would cause the

points to lie above the calculated curve. The position of the Pt AES data above the ideal growth curve is also indicative of an improper estimate of electron escape length for the Pt Auger electrons, since islanding would cause the points to lie below the calculated curve. At Pt coverages >3ML Fig.3 shows islanding to be more prominant since the Ti data points lie above and the Pt data points are more nearly on the calculated curve.

One might argue that ideal growth on a polycrystalline foil is not a valid concept. However, the data does qualitatively support ideal growth behavior in the low coverage regime. Though there is certainly some degree of islanding, our simple approach surely gives a close approximation for the mean Pt thickness in the system and shows that the degree of islanding is very similar on the oxidized and reduced substrates.

TDS after exposure to 0.6L H_2 at 120K for various amounts of Pt supported on TiO_2(ox) is shown in Fig. 4. This exposure was chosen to keep the background H_2 levels low and to eliminate ambiguities related to desorption from the sample mounting leads. These were particularly troublesome in determining desorption peaks for the lowest Pt coverages. We observed no change in desorption peak temperature, 300K, as a function of Pt overlayer thickness. Comparison of the H_2 desorption spectrum, taken at the highest Pt coverage, θ = 3.8ML, with desorption data from a variety of Pt surfaces shows good qualitative agreement. Desorption of H_2 from sputtered unannealed Pt(111) gives three H_2 desorption peaks (210, 310, and 380K).[14] Another Pt(111) study found H_2 desorption peaks at 293 and 230K.[15] H_2 TDS off polycrystalline Pt gave a broad desorption peak at 330K with shoulders at 240 and 380K.[16] These peak temperatures agree quite well with our multilayer Pt desorption spectra indicating satisfactory reliability in our TDS results. We observed no further change in either

peak position or integrated peak area for θ_{Pt} up to 6ML. These data indicate that bulk Pt properties for H_2 chemisorption are reached at ~ 3.5 ML on this fully oxidized surface.

Figure 4 also shows the TPD results of adsorption of 0.6L H_2 onto the platinized TiO_2(red) substrate. In contrast to the TiO_2(ox) sample there is a large, 75K, upward shift in the peak temperature as a function of Pt coverage. At high Pt coverages the spectra for both the oxicized and reduced forms become identical.

H_2 TDS peak areas as a function of Pt coverage are shown in Fig. 5 and are normalized to desorption from the high coverage, bulk Pt, case (P^o). For both samples the relative peak area increases linearly with Pt coverage at low Pt coverages. However, the oxidized sample has significantly greater affinity for hydrogen. For example, whereas the oxidized sample adsorbs nearly 70% of the bulk Pt quantity of hydrogen at θ_{Pt}=1.5ML, the reduced sample adsorbs only 22%. This tendency is also reflected in the coverage of Pt necessary to reach $P/P^o = 1$. The TiO_2(ox) sample reaches this point at 3.5 ML of Pt but the reduced sample requires 5ML. Reproducibility is quite satisfactory as is indicated by the results in Fig. 5 for two separate samples of TiO_2(red).

TDS experiments were also performed after the coadsorption of 0.6L H_2 followed by 1L CO at 120K (Fig. 6). Precoverage of hydrogen has no effect on the CO desorption spectrum and H_2 TDS will not be discussed further. In the CO TDS from the fully oxidized sample, a high temperature desorption peak (520K) grows as the Pt coverage increases and is saturated at θ_{Pt} = 1.5ML. There is also an upward shift (40K) in the low temperature, 440K, peak. Comparing our TDS results with results obtained from various Pt surfaces shows very reasonable agreement. CO desorption from

polycrystalline Pt gives four desorption peaks (115, 175, 415, and 507K).[16] Since we only cooled to 130K we did not observe the 115K desorption peak. There is a small peak near 180K but it is distorted by desorption from the leads. The high temperature peaks have roughly the same peak area ratios as that observed for polycrystalline Pt;[16] however, our peak temperatures are shifted by about 25K to higher values. Other CO on Pt desorption data is similar. Desorption peaks of 430 and 535K were observed for the Pt(110) surface.[17] Pt(111), 6(111)x(100) and 6(111)x(111) all give peaks at 420K and 530K.[18] These results support our interpretation of the data in terms of bulk Pt behavior at high Pt coverages.

Turning to the coadsorption of H_2 and CO on the partially reduced sample, a much larger coverage of Pt is necessary to acquire the high temperature CO desorption peak. Examination of Fig.6 shows that even at θ_{Pt} = 2.8 ML the high temperature CO peak is not present. Moreover, for θ_{Pt} = 4.4ML, the CO desorption has not acquired the bulk Pt TDS profile, as evidenced by the ratio of the two high temperature peaks. More desorption occurs in the 180-300K region on this reduced sample. The peak area of this low temperature region decreases almost linearly with increasing Pt coverage until θ_{Pt} = 2 ML. For higher Pt coverages the peak areas in the low temperature region are equal on the oxidized and reduced samples. Clearly, CO uptake is suppressed on the reduced sample.

By measuring the peak positions of both XPS and Auger transitions in the X-ray excited electron spectra, Auger parameters[19-22] were calculated for Pt/TiO_2(red) and Pt/TiO_2(ox) and are listed in Table I. These calculations are based on comparison of the data for θ_{Pt} = 0.5 and 8 ML, the latter coverage being equivalent to bulk Pt. The initial state chemical shift, ΔE, and final state relaxation shift, ΔR, are shown for the two different platinized subtrates. Values were calculated using the equations:

$$\Delta(BE) = \Delta E - \Delta R - \Delta E_{bending}$$

$$\Delta(KE) = - \Delta E + 3\Delta R + \Delta E_{bending}$$

where $\Delta E_{bending}$ represents the change in measured energy due to band bending. The validity of these equations has been the subject of much debate. Recent work indicates that corrections of up to 3 eV are warranted in some situations.[23] We will not attempt to address the accuracy of the simplifying assumptions from which these equations are derived. In spite of the difficulties of interpretation, the comparison of the two very similar systems discussed here is justified in the sense that differences in the values of ΔE will reflect different Pt/TiO_2 electronic structures.

As is evident from the data of Table I there is essentially no difference in the amount of initial state chemical shift for the two samples. $\Delta E_{bending}$, which would reflect changes in the underlying oxide in passing from low to high coverages of Pt, was assumed to be equal to zero for both the reduced and oxidized samples based on the fact that no BE change in either the Ti($2p_{3/2}$) or the valence levels (by UPS) were observed as the Pt coverage changed.

The quoted experimental error of ± 0.3 eV was obtained by simple propagation of error using 0.1 eV as the uncertainty in the XPS and AES measurements. Thus, we conclude that the difference in the amount of charge transfer in the two systems is negligible.

Discussion

The TDS experiments show that introduction of Ti^{3+} into the TiO_2 lattice has a large effect on the chemisorption properties of a Pt overlayer. Hydrogen chemisorption is suppressed and peak desorption temperatures are lowered when the substrate is reduced (Ti^{3+} is introduced) prior to Pt deposition. CO desorption profiles are also altered upon substrate reduction; a new low temperature desorption state appears and the highest temperature desorption peak disappears. These results are characteristic of SMSI and show that we have successfully modelled an SMSI catalyst.

Several explanations for the observed SMSI chemisorption effects have been offered. One involves contamination of the Pt overlayer. Carbon contamination can be a problem when vapor depositing Pt and small amounts of it can cause a significant change in the CO and H_2 desorption spectra. In earlier work[24] we reported neither CO nor H_2 chemisorption for Pt coverages of 3ML or less. With improved TDS sensitivity, these experiments were repeated and expanded in this work, and were shown to be in error due to C contamination in the Pt overlayer. Surface carbon has the dual effect of causing an error in the calibration of the Pt overlayer thickness and suppressing chemisorption. Contamination effects were successfully eliminated in the present experiments through a series of changes in the construction of the Pt doser. Careful AES analysis indicated no carbon

contamination.

Another postulated explanation for SMSI is the formation of Pt-TiC_x bonds and the consequent change in chemisorption because of alteration of the Pt atoms involved.[25] The results of Fig. 5 discount this as the direct and only cause. If a local Pt-Ti bond was responsible for the alteration in Pt chemisorption properties then the effect should extend over only 1-2ML of Pt. However, from Fig. 5 it is clear that the SMSI effect extends over more than 4ML since the curves(ox. and red.) do not coincide until coverages of at least 5ML of Pt are reached. This eliminates a local Pt-Ti bond as the sole cause for SMSI. This conclusion is supported by EXAFS data where no Pt-Ti or Pt-O bond distance could be observed with a coordination number greater than 0.5, the limit of EXAFS sensitivity.[26]

Another often postulated cause of SMSI is charge transfer from the support to the metal.[4,24,27] We detected no significant difference in the binding energy of the Pt core level when the reduced and oxidized substrates were compared and conclude that there is no support for a detectable difference in the oxidation number of Pt. This result is somewhat different from other work done on single cyrstal $SrTiO_3$[3] and for Ni/TiO_2 systems.[4] Our work is in good agreement with Huizinga[26] who finds no differences in reduced and oxidized Pt/TiO_2 powder systems by XPS. Huizinga suggests that the conclusions drawn in the $Pt/SrTiO_3$ and Ni/TiO_2 work mentioned above are the result of difficulties in the interpretation of calculated Auger parameters. It is worth noting that the extended range of the suppressed chemisorption indicated in Fig. 5 is strong evidence against the charge transfer model because charge screening lengths in metallic systems are no more than one lattice spacing.

TiO_2 migration and subsequent encapsulation of the Pt overlayer is a

fourth possible explanation for the observed SMSI effects. This effect could very well be a major contributor to SMSI in powder catalyst samples which have been subjected to long and high temperature reduction processes. However, the samples investigated here are not expected to be subject to this effect since the temperatures of Pt deposition were never higher than 300K. If encapsulation is occurring then it most likely happens as the hot gas phase Pt atoms strike the surface during deposition. We expect this would occur to about the same extent on both the reduced and oxidized samples since the near-surface region probably has about the same structure for both samples. Modeling of the experimental Pt AES growth curve was performed to determine the extent to which encapsulation could differ on the two different substrates without being detected. Very conservatively, these calculations indicate that the extent of migration could not exceed 0.25ML of TiO_2 in any case without being detectable. Thus, while we can not eliminate encapsulation on the reduced substrate as the cause of SMSI, it seems unlikely under our conditions.

In audition to encapsulation, other Pt overlayer morphology differences could exist. For the substrates prepared here, small differences in the amount of islanding or the structure of the islands could be a major contributor to SMSI. Since an oxidized polycrystalline Ti foil is used to support the Pt in our experiments, we do not expect long range order and/or ideal epitaxial growth of Pt on the substrate. Moreover, the local structure of the oxide surface is probably changed (both atomically and electronically) in passing from the fully oxidized to the partially reduced cases. Even though the AES growth curves (Fig. 3) show no significant differences in the two cases, this is not a strong constraint and the detailed local structure may be significantly different. If we attempt to

assign the differences in H_2 uptake(Fig. 1) observed at θ_{Pt}=1.5 ML solely to differences in 3L growth of Pt particles, then we must conclude that 70% fewer Pt atoms are exposed on the reduced surface. Differences in growth mode of this magnitude would certainly be detectable in the AES growth curves and we conclude that the suppression of chemisorption can not be attributed entirely to this cause.

Another difference in the Pt on the two supports could be the surface structure of the Pt particles as opposed to their overall size or thickness. Using electron microscopy, Baker et. al.[28,29] showed that Pt on reduced TiO_2 powder catalysts has a flat pillbox morphology as opposed to hemispherical particles on the oxidized catalyst.

The idea of a pillbox morphology on the reduced substrate is further supported by FTIR work done by Tanaka and White[30] who investigated CO stretching frequencies for CO adsorbed on both reduced and oxidized Pt/TiO_2 powders. Upon reduction, they observed preferential loss of a CO stretching frequency attributed to CO bound at step sites on Pt and argued that reduction of the catalyst lead to a Pt morphology dominated by close-packed (111) terrace sites. It is important to note that they also observed a decreased intensity in other CO stretching bands indicating an overall loss in CO uptake.

In light of these results, the following interpretation of our data is proposed. Pt deposited on the reduced surface tends to grow with a close-packed geometry whereas on the oxidized surface the tendency is toward rougher (higher Miller index) surfaces. These modes are governed by small changes in the character of the Pt/TiO_2 interaction at very low coverages. These initial interaction differences, which are assumed to control the kind of metal surface structure formed, become insignificant only after several

ML of Pt have been deposited. Now assume that the high temperature (570K) CO desorption peak can be attributed to desorption of CO from step sites. This assumption is based on HREELS and TDS work by McClellan and Gland for CO adsorption on a Pt(321) surface.[31] They attribute a high temperature(546K) CO desorption state to desorption from step sites. On this basis, one would expect high temperature peaks to be stronger on oxidized than reduced samples as observed. As is evident from Fig. 6, more than 3ML of Pt are required before a high temperature CO desorption state is seen for the reduced TiO_2 sample.

These morphology differences, by themseleves, can not account for all the observations. Nonstepped Pt surfaces such as Pt(111) and Pt(110) have desorption states in the 400-550K region.[17,18] Therefore, even if the Pt overlayer morphology changes to the flatter structure upon reduction, it should still show CO desorption in the high temperature regime. To account for the full loss of the high temperature CO desorption on the reduced samples, we propose that there is, particulary at low coverages, an electronic interaction between the Pt and the reduced support that alters slightly the state of the Pt and lowers the strength of the Pt-CO bond. Our XPS data shows that this interaction cannot be explained as simple charge transfer between support and metal. Using UPS and ELS we were unable to detect any significant differences in the valence electronic stucture of the oxidized and reduced Pt/TiO_2 systems, but further work with better sensitivity and resolution is needed. The electronic effects seem to be fairly short-ranged as evidenced by monitoring the peak area of the low temperature CO desorption peaks. At Pt coverages of 2ML the low temperature desorption region for the reduced sample is the same as for bulk Pt (both shape and area). This can be taken as a rough guide to the extent of the

interaction. While these electronic and morphology changes occur simultaneously, further speculation about their origin and interrelation is not warranted.

Conclusions

From the data presented here we draw the following conclusions:

1) An SMSI catalyst can be successfully modelled using low surface area thin films of oxidized Ti metal with controlled amounts of Pt vapor-deposited thereon.

2) Suppression of CO and H_2 chemisorption on reduced, as compared to fully oxidized titania films with Pt overlayers, is interpreted in terms of two factors: (a) flatter Pt particle morphology on the reduced samples and (b) a different electronic interaction between the Pt and TiO_2 which, at low Pt coverages, suppresses CO and H_2 chemisorption.

3) Auger parameter measurements indicate that the electronic interaction is not the result of a simple charge transfer.

References

1. S.J. Tauster, S.C. Fung, and R.L. Garten, J. Amer. Chem. Soc., 100,170(1978).
2. S.J. Tauster and S.C. Fung, J. Catal., 55,29(1978).
3. M.K. Bahl, S.C. Tsai, and Y.W. Chung, Phys. Rev. B21,1344(1980).
4. C.C. Kao, S.C. Tsai, and Y.W. Chung, J. Catal., 73,136(1982).
5. C.C. Kao, S.C. Tsai, M.K. Bahl, and Y.W. Chung, Surface Sci., 95,1(1980).
6. J.W. Rogers, C.T. Campbell, R.L. Hance, and J.M. White, Surface Sci., 97,425(1980).
7. C.D. Wagner, W.M. Riggs, L.E. Davis, J.F. Moulder, and G.E. Mullenberg, Handbook of X-ray Photoelectron Spectroscopy (Physical Electronics Ind., Inc., 1979)p.68.
8. M.P. Seah and W.A. Tench, Surface and Interface Analysis, 1,2(1979).
9. E.I. Ko and R.J. Madix, Surface Sci., 100,L449(1980)
10. M. Kiskinova and D.W. Goodman, Surface Sci., 109,L555(1981).
11. D. J. Jackson, T. E. Gallon, and A. Chambers, Surface Sci., 36,381(1973).
12. C.C. Chung, Surface Sci., 48,9(1975).
13. M.L. Tarng and G.K. Wehner, J. Appl. Phys., 44,1534(1973).
14. K. Christmann, G. Ertl, and T. Pignet, Surface Sci., 54,365(1976).
15. K. Christmann and G. Ertl, Surface Sci., 60,365(1976).
16. K.T. Thrush and J.M. White unpublished.
17. R.W. McCabe and L.D. Schmidt, Surface Sci., 60,85(1976).
18. D.M.Collins and W.E. Spicer, Surface Sci., 69,55(1977).

19. C.D. Wagner and P. Biloen, Surface Sci., 35,82(1973).

20. T.D. Thomas, J. Electron Spec. and Relat. Phenom., 20,117(1980).

21. N.D. Lang and A.R. Williams, Phys. Rev. B16,2408(1977).

22. S.P. Kowalczyk, L. Ley, F.R. McFeely, R.A. Pollak, and D.A. Shirley, Phys. Rev. B9,381(1974).

23. T.D. Thomas, J. Electron Spec. Relat. Phenom., 20,117(1980).

24. J.A. Schreifels, D.N. Belton, J.M. White and R.L. Hance, Chem. Phys. Lett., 90,261(1982).

25. J.A. Horsely, J. Amer. Chem. Soc., 110,2870(1979).

26. T. Huizinga, Metal Suppport Interactions in Pt and Rh Al_2O_3 and TiO_2 Catalysts. Dissertation, Eindhoven University of Technology,(1983).

27. B.H. Chen and J.M. White, J. Phys. Chem., 86,3534(1982).

28. R.T.K. Baker, E.B. Prestridge, and R.L. Garten, 59,293(1979).

29. R.T.K.Baker, J. Catal., 63,523(1980).

30. K. Tanaka and J.M. White, J. Catal., 79,81(1983).

31. M.R. McClellan, F.R. McFeely and J.L. Gland, G.M. Research Report PC-182(1981).

TABLE I

Substrate	ΔBE(eV)[a]	ΔKE(eV)	ΔE(eV)	ΔR(eV)
TiO_2(ox)	+ 0.5	- 1.4	+ 0.1	- 0.45
TiO_2(red)	+ 0.4	- 1.4	- 0.1	- 0.5

a. ΔBE and ΔKE are calculated by taking the difference between measurements for θ_{Pt} = 8 and 0.5 ML.

Figure Captions

Figure 1: XPS of Ti(2p) region for TiO_2(ox) and TiO_2(red).

Figure 2: AES of multilayer Pt deposited on TiO_2(ox).

Figure 3: Ti(387), open symbols, and Pt(235), closed symbols, AES signals vs. Pt dose on TiO_2(ox), triangles, and TiO_2(red), circles. Calculated ideal growth(layer-by-layer) curve is indicated by the solid curves.

Figure 4: H_2 TDS of 0.6L H_2 adsorbed at 130K. Each spectrum is labeled with coverage of Pt (ML) deposited on the TiO_2 substrate prior to the desorption experiment.

Figure 5: Relative peak areas for H_2 desorption from platinized TiO_2(ox),triangles, and TiO_2(red), circles. Filled and open circles represent 2 different experiments on TiO_2(red). Adsorption conditions were the same as for Fig. 4.

Figure 6: CO TDS of 1L CO coadsorbed with 0.6L H_2 at 130K. Each spectrum is labelled with the coverage of Pt deposited onto the TiO_2 substrate prior to the desorption experiment.

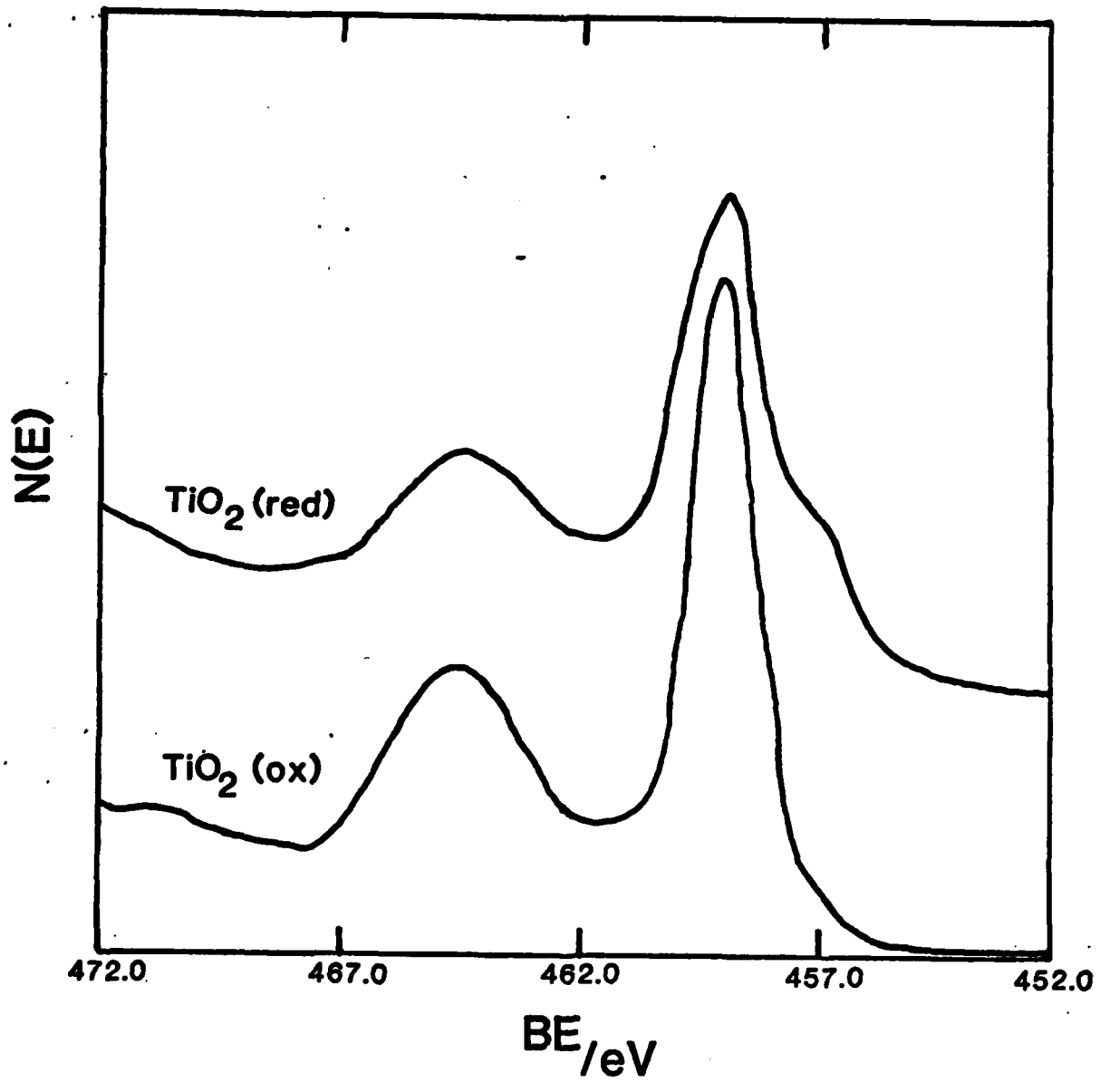
N(E)
TiO2 (red)
TiO2 (ox)
472.0
467.0
462.0
457.0
452.0
BE/eV

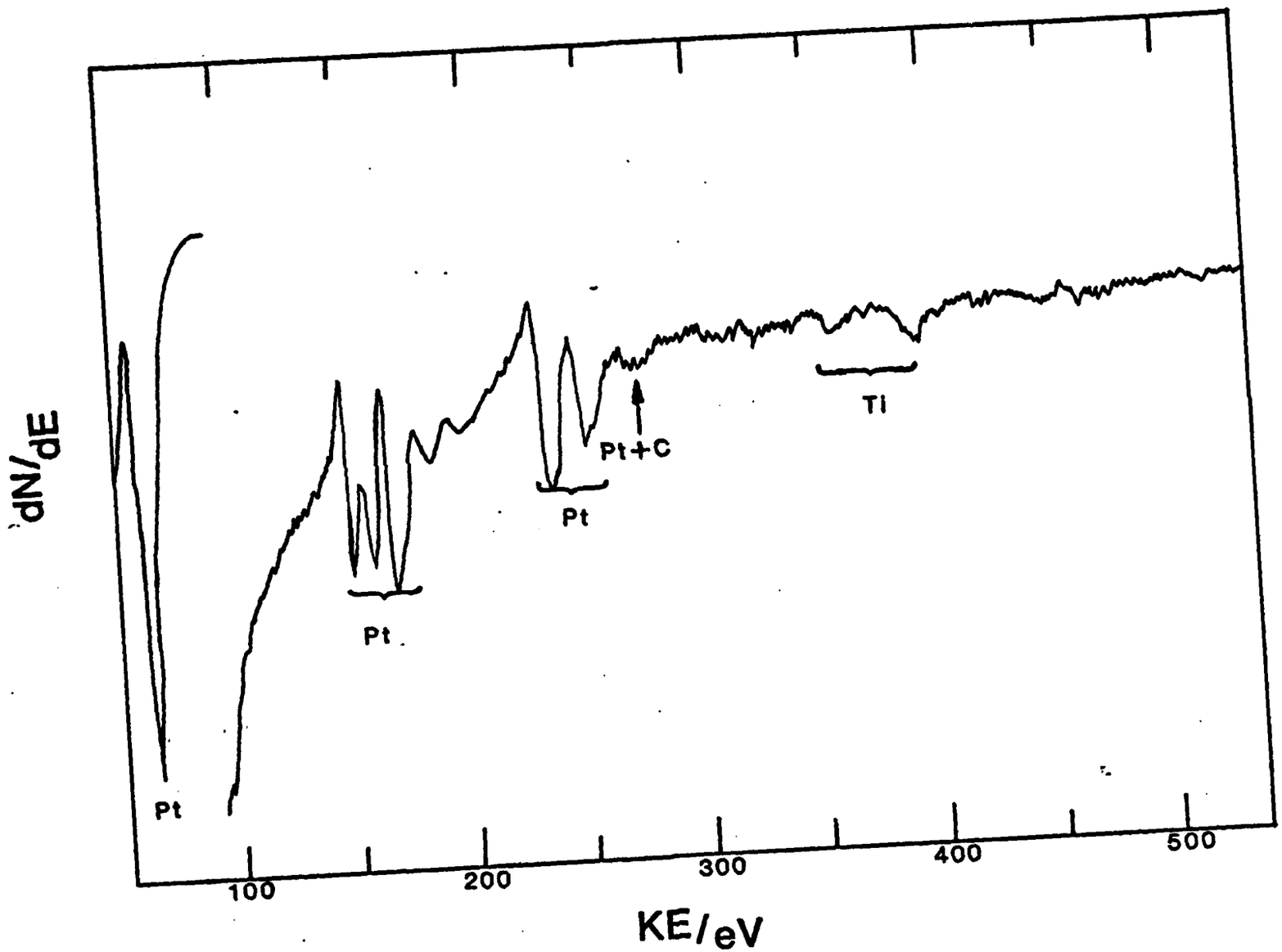
dN/dE
Pt
Pt
Pt
Pt+C
Tl
100
200
300
400
500
KE/eV

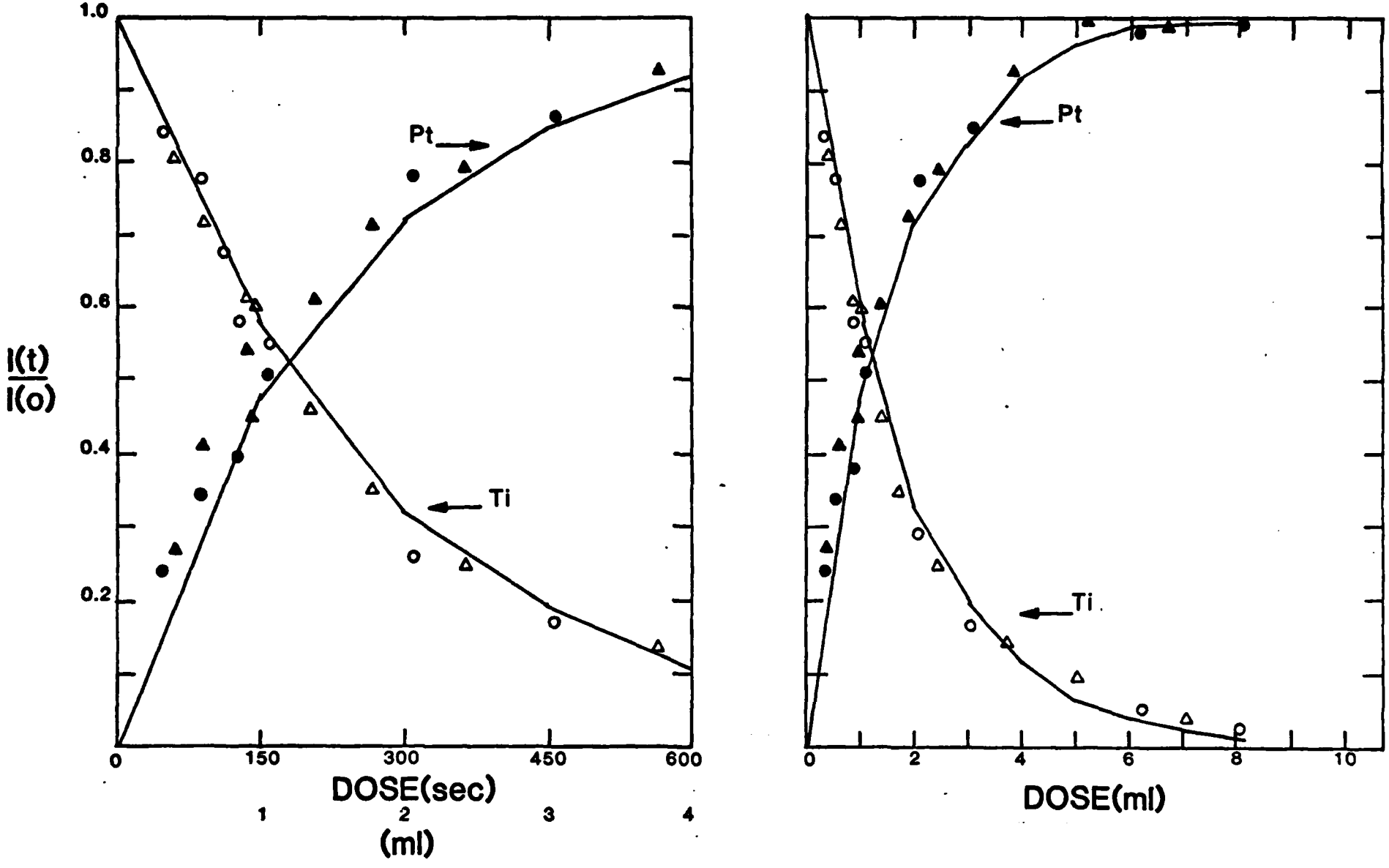
1.0
0.8
0.6
0.4
0.2
I(t)/I(o)
Pt
Ti
0
150
300
450
600
DOSE(sec)
1
2
3
4
(ml)
Pt
Ti
0
2
4
6
8
10
DOSE(ml)

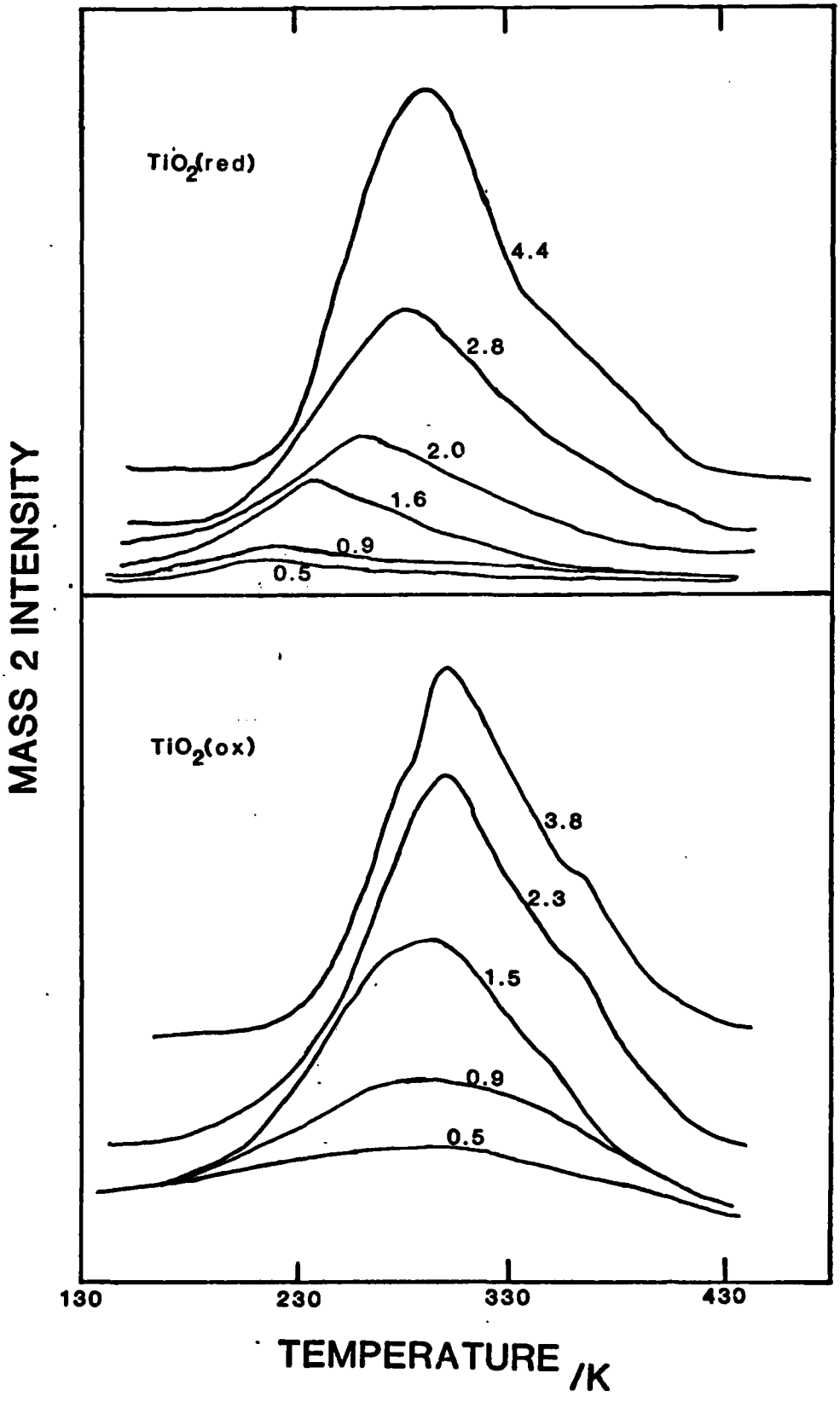
TiO2(red)
4.4
2.8
2.0
1.6
0.9
0.5
TiO2(ox)
3.8
2.3
1.5
0.9
0.5
MASS 2 INTENSITY
130
230
330
430
TEMPERATURE /K

Fig 4

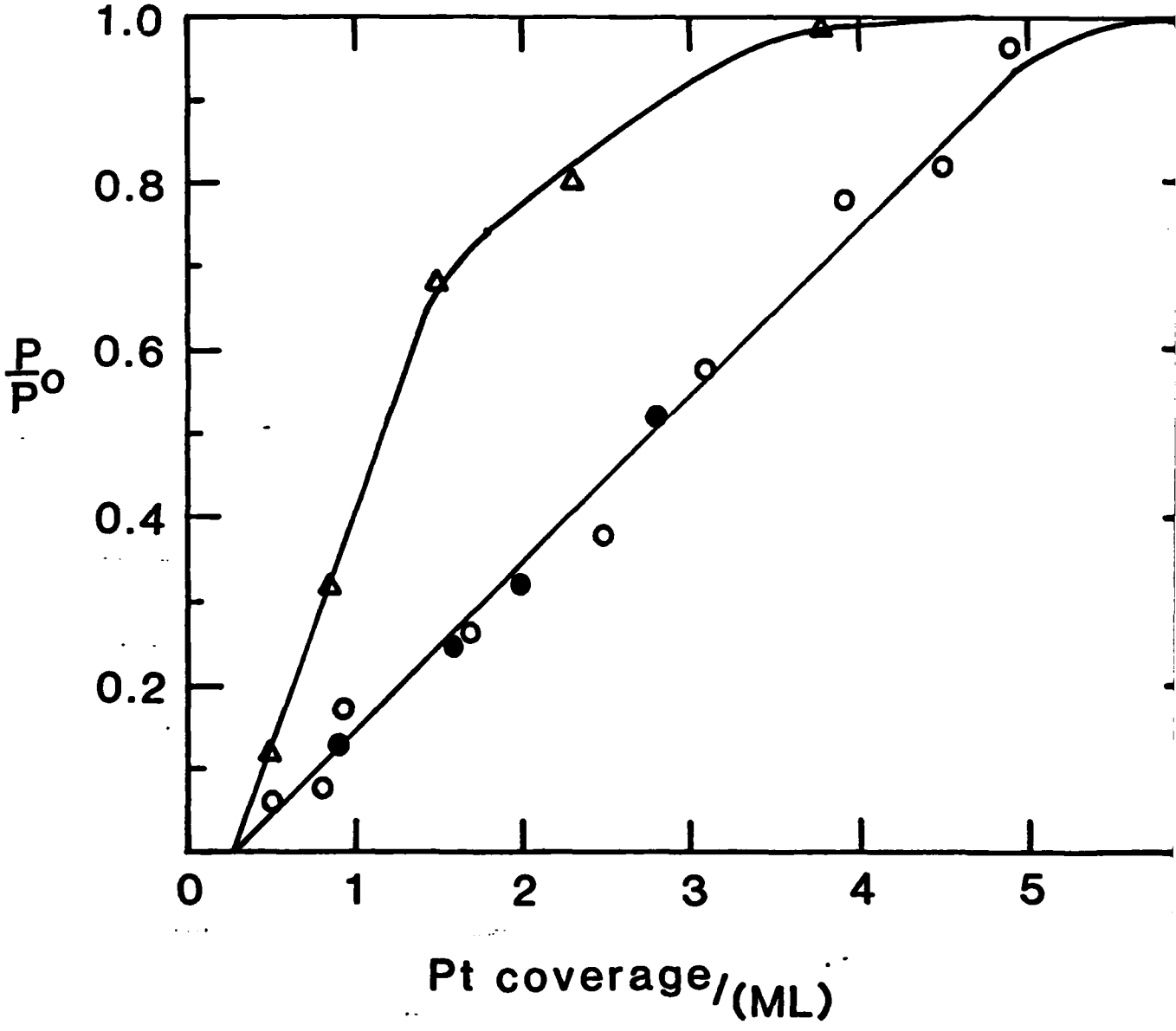

Fig 5

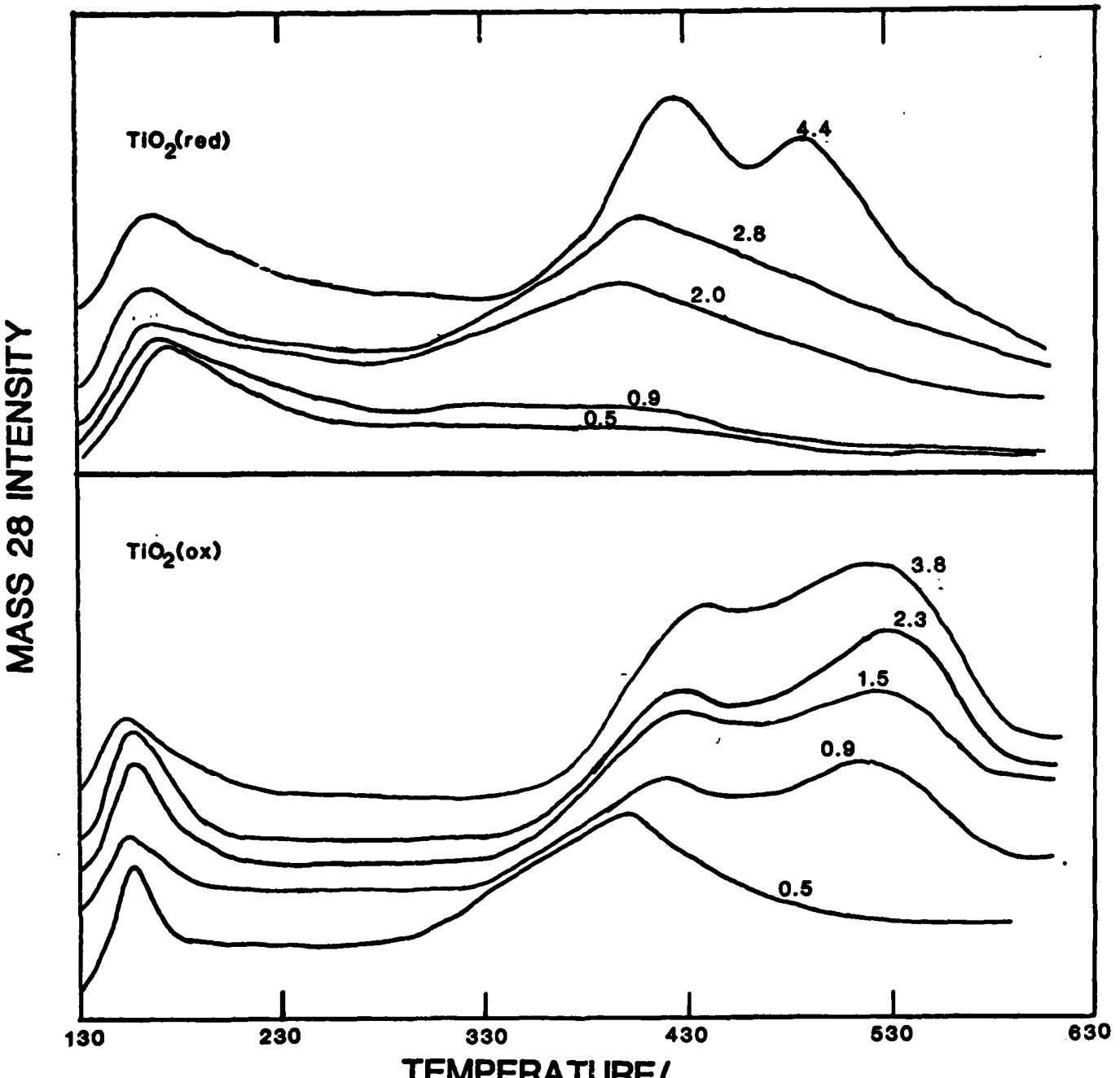
TiO2(red)
4.4
2.8
2.0
0.9
0.5
TiO2(ox)
3.8
2.3
1.5
0.9
0.5
MASS 28 INTENSITY
130
230
330
430
530
630
TEMPERATURE/K

Fig

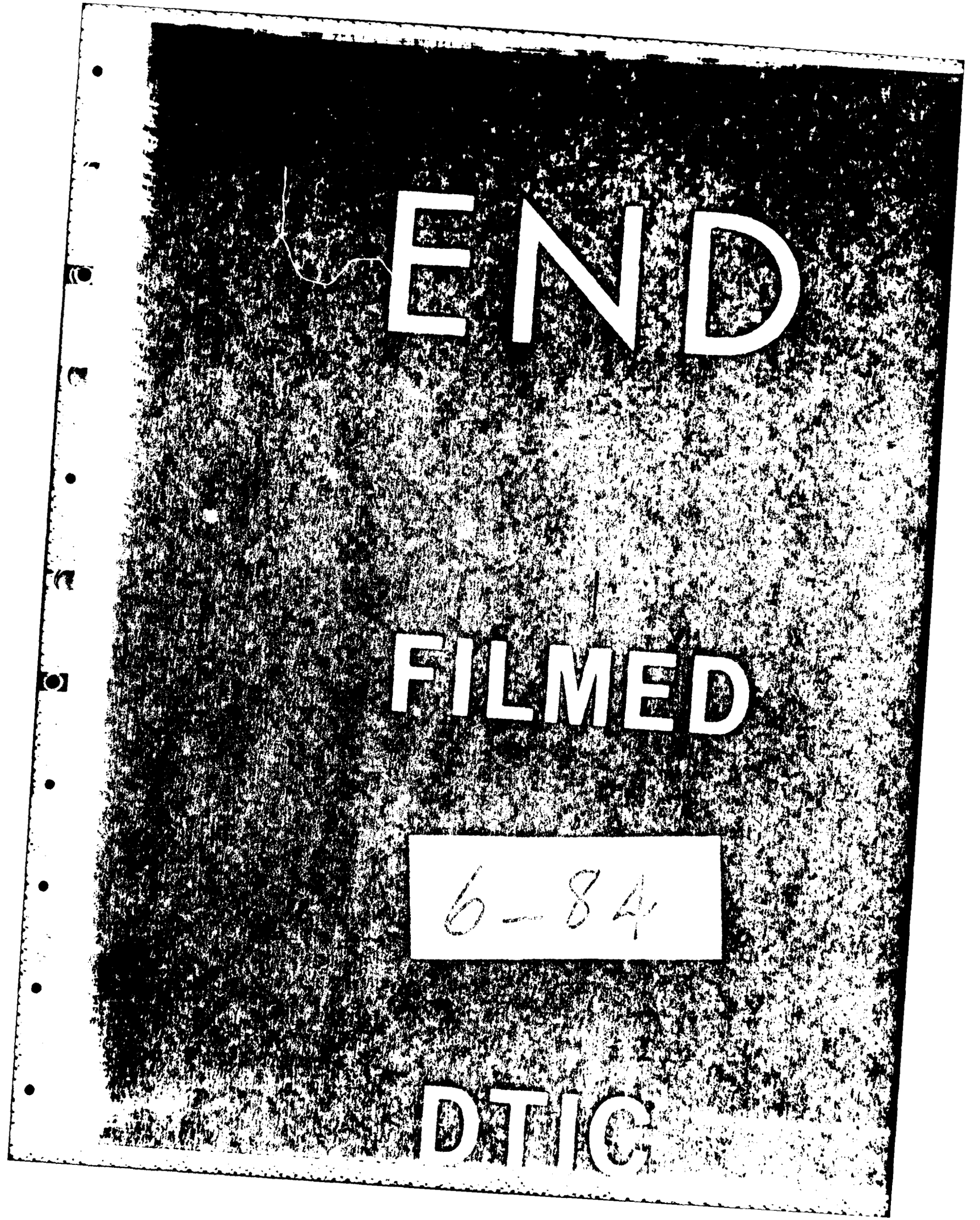
END
FILMED
6-84
DTIC